

Tracking Control of a Spherical Inverted Pendulum with an Omnidirectional Mobile Robot*

Sho-Tsung Kao

Department of Engineering Science
National Cheng Kung University
Tainan City, Taiwan

Ming-Tzu Ho

Department of Engineering Science
National Cheng Kung University
Tainan City, Taiwan
bruceho@mail.ncku.edu.tw

Abstract—This paper considers the problems of design and implementation of trajectory tracking control of a spherical inverted pendulum with an omni-directional mobile robot. The control objective is to control the robot to track the desired translational trajectory with desired orientation while maintaining the inverted pendulum in its upright position. The mathematical models of the spherical pendulum and omni-directional mobile robot are given to facilitate the control analysis and design. Based on linear output regulation, and inverse dynamics, a tracking controller is designed to achieve asymptotic trajectory and orientation tracking. The designed control law is implemented on a digital signal processor and tested on an experimental apparatus. The effectiveness of the designed control scheme is validated through experimental studies. The results show that the robot is able to track the reference trajectory and reference orientation while balancing the inverted pendulum.

Keywords—*Spherical inverted pendulum; Omnidirectional mobile robot; Tracking control; Output regulation*

I. INTRODUCTION

The inverted pendulum model resembles many simplified systems that arise in robotic and aerospace applications. The control of an inverted pendulum is a well-known challenging control problem. Because of their inherent nonlinearity, instability, and underactuation, these inverted pendulum systems are widely used as a benchmark for verifying the performance and effectiveness of new control algorithms or technology. A spherical inverted pendulum is a rod attached to a horizontal movable base with a universal joint. The movable base is free to move on the plane acted on by a planar control force. It is a two-dimensional inverted pendulum. A variety of control methods [1]-[4] have been used to stabilize a spherical inverted pendulum at its upright equilibrium. Many studies have experimentally validated the stabilization of a spherical inverted [5]-[8]. In [5]-[7], an X - Y table was used to provide the controlled planar force. In [8], the spherical inverted pendulum was actuated by a SCARA robot.

Due to their structural simplicity and highly static stability, wheels are by far the most commonly used locomotion mechanism in mobile robotic applications. There are various types of wheeled mobile robots. Among them, the omnidirectional wheeled mobile robot can perform translational movement along any desired path combined with any rotational

movement. This wheeled mobile robot has superior maneuverability and has recently attracted a lot of attention in industrial applications and academic research [9]-[13]. In our work [14], we have successfully designed and implemented balance control of a spherical inverted pendulum actuated by an omni-directional mobile robot.

The problem of output regulation [15] is to control the system to achieve asymptotic tracking of prescribed trajectories and/or asymptotic rejection of undesired disturbances while maintaining closed-loop stability. Output regulation is one of the most important and fundamental problems in control theory and applications. Theoretical developments of the linear output regulation can be found in [15]-[19]. The studies of output regulation for a spherical inverted pendulum system were reported in [20, 21], in which the designed control schemes were validated through numerical simulations only.

This paper is to design and implement trajectory and orientation tracking control of a spherical inverted pendulum with an omni-directional mobile robot. The mathematical models of the spherical inverted pendulum and omni-directional mobile robot are given to facilitate the control design. Based on linear output regulation, and inverse dynamics, the tracking controller is designed to achieve asymptotic trajectory and orientation tracking. The designed control law is implemented and tested on an experimental apparatus. The effectiveness of the controllers is validated through simulation and experimental studies.

The rest of this paper is organized as follows. In Section II, The mathematical models of the spherical inverted pendulum and omni-directional mobile robot are given. In Section III, reviews the design methodology of linear out regulation. The tracking controller design is presented in Section IV. A brief description of the experimental setup is given in Section V. In Section VI, the experimental results are presented. Finally, Section VII contains some concluding remarks.

II. MATHEMATICAL MODELS

A. Model of a Spherical Inverted Pendulum

This subsection presents the system model of a spherical inverted pendulum. Basic features of a spherical inverted pendulum are illustrated in Fig. 1. The coordinate system $OXYZ$ denotes the world frame and ox_p, y_p, z_p is the body

*This work was supported by the Ministry of Science and Technology of Taiwan under Grant NSC 102-2221-E-006-209.

frame attached to the pendulum with the origin located at the center of mass of the robot. In addition to horizontal movement, the omni-directional mobile robot is also able to rotate about the Z-axis. Thus, the rotational movement has to be taken into consideration.

The parameters of the system are defined as follows:

m : mass of the pendulum.

M : mass of the mobile robot.

I_{czz} : moment of inertia of the robot about the Z-axis.

l : length of the pendulum.

x, y : position of the center of mass of the robot with respect to the X and Y -axes, respectively.

β, α, ϕ : angular displacement of the pendulum about the X , Y , and Z directions, respectively.

$I_{pxx}, I_{pyy}, I_{pzz}$: moment of inertia of the pendulum about the x_p, y_p , and z_p -axes, respectively.

g : gravitational acceleration.

F_x : control force exerted in the X -axis.

F_y : control force exerted in the Y -axis.

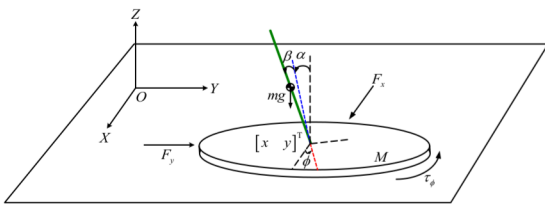


Fig. 1 Spherical inverted pendulum.

Based on the Euler-Lagrange formulation [23], the dynamic equations of the system are given by

$$(m+M)\ddot{x} + ml[\ddot{\alpha} \cos \alpha \cos \beta \cos \phi - \ddot{\beta}(\sin \alpha \sin \beta \cos \phi + \cos \beta \sin \phi) - \ddot{\phi}(\sin \alpha \cos \beta \cos \phi + \sin \beta \cos \phi) - \dot{\alpha}^2 \sin \alpha \cos \beta \cos \phi + \dot{\beta}^2(\sin \beta \sin \phi - \sin \alpha \cos \beta \cos \phi) + \dot{\phi}^2(\sin \beta \sin \phi - \sin \alpha \cos \beta \cos \phi) - 2\dot{\alpha}\dot{\beta} \cos \alpha \sin \beta \cos \phi - 2\dot{\alpha}\dot{\phi} \cos \alpha \cos \beta \sin \phi + 2\dot{\beta}\dot{\phi}(\sin \alpha \sin \beta \sin \phi - \cos \beta \cos \phi)] = F_x, \quad (1)$$

$$m[\ddot{x} \cos \alpha \cos \beta \cos \phi + \ddot{y} \cos \alpha \cos \beta \sin \phi + l^2 \ddot{\alpha} \cos^2 \beta - l^2 \ddot{\phi} \cos \alpha \sin \beta \cos \beta - l^2 \ddot{\phi}^2 \sin \alpha \cos \alpha \cos^2 \beta - 2l^2 \dot{\alpha}\dot{\beta} \sin \beta \cos \beta - 2l^2 \dot{\beta}\dot{\phi} \cos \alpha \cos^2 \beta + \ddot{\phi}(\cos^2 \beta I_{pyy} + \sin^2 \beta I_{pzz}) + \dot{\phi} \cos \alpha \sin \beta \cos \beta (-I_{pyy} + I_{pzz}) + \dot{\phi}^2 \sin \alpha \cos \alpha (-I_{pxx} + \sin^2 \beta I_{pyy} + \cos^2 \beta I_{pzz}) + 2\dot{\alpha}\dot{\beta} \sin \beta \cos \beta (-I_{pyy} + I_{pzz}) + \dot{\beta}\dot{\phi} \cos \alpha (-I_{pxx} + \sin^2 \beta I_{pyy} - \cos^2 \beta I_{pyy} - \sin^2 \beta I_{pzz} + \cos^2 \beta I_{pzz}) - mg \sin \alpha \cos \beta] = F_y, \quad (2)$$

$$(m+M)\ddot{y} + ml[\ddot{\alpha} \cos \alpha \cos \beta \sin \phi + \ddot{\beta}(\cos \beta \cos \phi - \sin \alpha \sin \beta \sin \phi) + \ddot{\phi}(\sin \alpha \cos \beta \cos \phi - \sin \beta \sin \phi) - \dot{\alpha}^2 \sin \alpha \cos \beta \sin \phi - \dot{\beta}^2(\sin \alpha \cos \beta \sin \phi + \sin \beta \cos \phi) - 2\dot{\alpha}\dot{\beta} \cos \alpha \sin \beta \sin \phi + 2\dot{\alpha}\dot{\phi} \cos \alpha \cos \beta \cos \phi - 2\dot{\beta}\dot{\phi}(\sin \alpha \sin \beta \cos \phi + \cos \beta \sin \phi)] = F_y, \quad (3)$$

$$m[-l\ddot{x}(\sin \alpha \sin \beta \cos \phi + \cos \beta \sin \phi) + l\ddot{y}(\cos \beta \cos \phi - \sin \alpha \sin \beta \sin \phi) - l^2 \ddot{\alpha} \cos \alpha \sin \beta \cos \phi + l^2 \ddot{\phi} \sin \alpha + l^2 \dot{\alpha}^2 \sin \beta \cos \phi - l^2 \dot{\phi}^2 \cos^2 \alpha \sin \beta \cos \phi + 2l^2 \dot{\alpha}\dot{\phi} \cos \alpha \cos^2 \beta] + I_{pxx}\ddot{\beta} + I_{pox}\dot{\phi} \sin \alpha + \dot{\alpha}^2 \sin \beta \cos \beta (-I_{pyy} + I_{pzz}) + \dot{\phi}^2 \cos^2 \alpha \sin \beta \cos \beta (-I_{pyy} + I_{pzz}) + \dot{\alpha}\dot{\phi} \cos \alpha (I_{pxx} + \cos^2 \beta I_{pyy} - \sin^2 \beta I_{pzz}) - \sin^2 \beta I_{pyy} - \cos^2 \beta I_{pzz} + \sin^2 \beta I_{pzz} - mgl \cos \alpha \sin \beta = 0, \quad (4)$$

$$m[-l\ddot{x}(\sin \beta \cos \phi + \sin \alpha \cos \beta \sin \phi) + l\ddot{y}(\sin \alpha \cos \beta \cos \phi - \sin \beta \sin \phi) - l^2 \ddot{\alpha} \cos \alpha \sin \beta \cos \phi + l^2 \ddot{\phi} (\sin^2 \alpha \cos^2 \beta + \sin^2 \beta) + l^2 \dot{\alpha}^2 \sin \alpha \sin \beta \cos \phi + l^2 \dot{\phi} \cos \alpha \sin \beta \cos \phi + 2l^2 \dot{\alpha}\dot{\beta} \cos \alpha \sin^2 \beta + 2l^2 \dot{\alpha}\dot{\phi} \sin \alpha \cos \alpha \cos^2 \beta + 2l^2 \dot{\beta}\dot{\phi} \cos \alpha \sin \alpha \cos \alpha \cos^2 \beta + 2l^2 \dot{\beta}\dot{\phi} \cos^2 \alpha \sin \beta \cos \beta (-I_{pyy} + I_{pzz}) + \ddot{\alpha} \cos \alpha \sin \beta \cos \beta (-I_{pyy} + I_{pzz}) + \ddot{\beta} \sin \alpha I_{pxx} + \dot{\phi} (\sin^2 \alpha I_{pxx} + \cos^2 \alpha \sin^2 \beta I_{pyy} + \cos^2 \alpha \cos^2 \beta I_{pzz} + I_{czz}) + \dot{\alpha}^2 \sin \alpha \sin \beta \cos \beta (I_{pyy} - I_{pzz}) + \dot{\alpha}\dot{\beta} \cos \alpha (I_{pxx} - \cos^2 \beta I_{pyy} + \sin^2 \beta I_{pyy} + \cos^2 \beta I_{pzz} - \sin^2 \beta I_{pzz}) + 2\dot{\alpha}\dot{\phi} \sin \alpha \cos \alpha (I_{pxx} - \sin^2 \beta I_{pyy} - \cos^2 \beta I_{pzz}) + 2\dot{\beta}\dot{\phi} \cos^2 \alpha \sin \beta \cos \beta (I_{pyy} - I_{pzz}) = \tau_\phi. \quad (5)$$

B. Model of an Omni-directional Mobile Robot

The top view of a mobile robot is illustrated in Fig. 2. Three wheels are equally spaced at 120° from one another. It is assumed that there is no slip in all wheels. Here, OXY is the world frame and $oX_m Y_m$ is the body frame attached to the robot with the Y_m -axis aligned with respect to wheel 1.

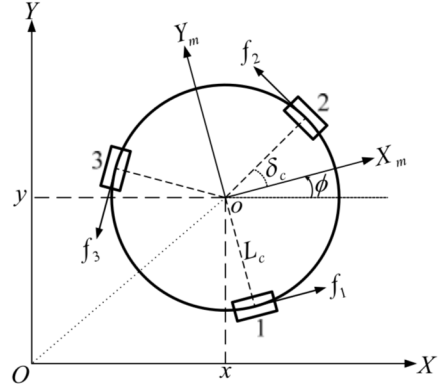


Fig. 2 Top view of omni-directional mobile robot.

The system parameters of the omni-directional mobile robot are defined as follows:

M_t : mass of the robot with the pendulum.

L_c : radius of the robot.

f_1, f_2, f_3 : traction force of the ground on wheels 1, 2, and 3, respectively.

R_w : radius of the wheels.

δ_c : orientation of wheel 2 with respect to the X_m -axis and $\delta_c = 30^\circ$.

$\theta_1, \theta_2, \theta_3$: angular displacement of wheels 1, 2, and 3, respectively.

$\omega_1, \omega_2, \omega_3$: angular velocity of wheels 1, 2, and 3, respectively.

The dynamic equations of the omni-directional mobile robot [9] are given by

$$\begin{bmatrix} \ddot{x} \\ \ddot{y} \\ \ddot{\phi} \end{bmatrix} = \begin{bmatrix} M_t & 0 & 0 \\ 0 & M_t & 0 \\ 0 & 0 & I_{pxz} + I_{czz} \end{bmatrix} \begin{bmatrix} \cos\phi & -\sin\phi & 0 \\ \sin\phi & \cos\phi & 0 \\ 0 & 0 & 1 \end{bmatrix} \begin{bmatrix} 1 & -\frac{1}{2} & -\frac{1}{2} \\ 0 & \frac{\sqrt{3}}{2} & -\frac{\sqrt{3}}{2} \\ L_c & L_c & L_c \end{bmatrix} \begin{bmatrix} f_1 \\ f_2 \\ f_3 \end{bmatrix}. \quad (6)$$

The kinematic equations of the omni-directional mobile robot [9] are

$$\begin{bmatrix} \omega_1 \\ \omega_2 \\ \omega_3 \end{bmatrix} = \frac{1}{R_w} \begin{bmatrix} 1 & 0 & L_c \\ -\frac{1}{2} & \frac{\sqrt{3}}{2} & L_c \\ -\frac{1}{2} & -\frac{\sqrt{3}}{2} & L_c \end{bmatrix} \begin{bmatrix} \cos\phi & \sin\phi & 0 \\ -\sin\phi & \cos\phi & 0 \\ 0 & 0 & 1 \end{bmatrix} \begin{bmatrix} \dot{x} \\ \dot{y} \\ \dot{\phi} \end{bmatrix}. \quad (7)$$

Since the electrical time constant of a motor is usually much smaller than the mechanical time constant and the value of the viscous friction coefficient is negligible, the following reduced-order model of the dc motor is adopted

$$\tau_m = \frac{K_t}{R_a} u - \frac{K_t^2}{R_a} \omega_m \quad (8)$$

where τ_m is the motor torque, u is the control voltage, K_t is the motor torque constant, ω_m is the angular velocity of the motor, and R_a is the armature resistance. The relationship between the motor torque and the force f is given by

$$f = \frac{1}{R_w} \tau_m, \quad (9)$$

It is assumed that three dc motors are identical. From (8) and (9), we have

$$\begin{bmatrix} f_1 \\ f_2 \\ f_3 \end{bmatrix} = \frac{K_t}{R_w R_a} \begin{bmatrix} u_1 \\ u_2 \\ u_3 \end{bmatrix} - \frac{K_t^2}{R_w R_a} \begin{bmatrix} \omega_1 \\ \omega_2 \\ \omega_3 \end{bmatrix}, \quad (10)$$

where u_1, u_2 , and u_3 are the control voltages of the three motors, respectively. From (6), (7), and (10), the dynamics of the robot with motors can be written as

$$\ddot{P}_w = A_w \dot{P}_w + B_w(\phi) U_C, \quad (11)$$

where

$$\begin{aligned} P_w &= [x \ y \ \phi]^T, \quad U_C = [u_1 \ u_2 \ u_3]^T, \\ A_w &= \begin{bmatrix} a_1 & 0 & 0 \\ 0 & a_1 & 0 \\ 0 & 0 & a_2 \end{bmatrix}, \end{aligned} \quad (12)$$

$$B_w(\phi) = \begin{bmatrix} 2b_1 \cos(\phi) & -b_1 \cos(\phi) - \sqrt{3}b_1 \sin(\phi) & -b_1 \cos(\phi) + \sqrt{3}b_1 \sin(\phi) \\ 2b_1 \sin(\phi) & -b_1 \sin(\phi) + \sqrt{3}b_1 \cos(\phi) & -b_1 \sin(\phi) - \sqrt{3}b_1 \cos(\phi) \\ b_2 & b_2 & b_2 \end{bmatrix}, \quad (13)$$

with

$$a_1 = \frac{-3K_t^2}{2R_w^2 M_t R_a}, \quad a_2 = \frac{-3K_t^2 L_c^2}{R_w^2 I_z R_a}, \quad b_1 = \frac{K_t}{2R_w M_t R_a}, \quad b_2 = \frac{K_t L_c}{R_w I_z R_a}. \quad (14)$$

Using inverse dynamics we obtain the following relationship between the control forces and control voltages

$$\begin{bmatrix} u_1 \\ u_2 \\ u_3 \end{bmatrix} = \begin{bmatrix} \frac{\cos\phi}{3b_1} (\frac{F_x}{M_t} - a_1 \dot{x}) & + \frac{\sin\phi}{3b_1} (\frac{F_y}{M_t} - a_1 \dot{y}) & + \frac{\tau_\phi}{I_{pxz} + I_{czz}} - a_2 \dot{\phi} \\ -\frac{\sqrt{3} \sin\phi - \cos\phi}{6b_1} (\frac{F_x}{M_t} - a_1 \dot{x}) & -\frac{\sqrt{3} \cos\phi + \sin\phi}{6b_1} (\frac{F_y}{M_t} - a_1 \dot{y}) & + \frac{\tau_\phi}{I_{pxz} + I_{czz}} - a_2 \dot{\phi} \\ -\frac{\sqrt{3} \sin\phi - \cos\phi}{6b_1} (\frac{F_x}{M_t} - a_1 \dot{x}) & -\frac{\sqrt{3} \cos\phi + \sin\phi}{6b_1} (\frac{F_y}{M_t} - a_1 \dot{y}) & + \frac{\tau_\phi}{I_{pxz} + I_{czz}} - a_2 \dot{\phi} \end{bmatrix}. \quad (15)$$

Once the planar control forces F_x , F_y , and τ_ϕ are obtained, (15) is used to determine the control voltage of each motor.

III. LINEAR OUTPUT REGULATION

Consider a linear time-invariant system

$$\begin{aligned} \dot{z}(t) &= Az(t) + Bu(t) + E_d d(t), \\ y(t) &= Cz(t) + Du(t) + F_d d(t), \end{aligned} \quad (16)$$

where $z(t)$ is the system state, $u(t)$ is the system input, $y(t)$ is the system output, $d(t)$ is a disturbance, A , B , E_d , C , D , and F_d are matrices of appropriate dimensions. Let $r(t)$ denote the reference input. Thus, the tracking error is given by

$$\begin{aligned} e(t) &= y(t) - r(t) \\ &= Cz(t) + Du(t) + F_d d(t) - r(t). \end{aligned} \quad (17)$$

Let the reference input and disturbance are generated by the following autonomous systems

$$\begin{aligned} \dot{r}(t) &= A_{lr} r, \quad r(0) = r_0, \\ \dot{d}(t) &= A_{ld} d(t), \quad d(0) = d_0 \end{aligned} \quad (18)$$

Then we obtain the exosystem [15] given by

$$\dot{v}(t) = A_l v(t), \quad v(0) = \begin{bmatrix} r_0 \\ d_0 \end{bmatrix} \quad (19)$$

where

$$v(t) = \begin{bmatrix} r(t) \\ d(t) \end{bmatrix}, A_l = \begin{bmatrix} A_{lr} & 0 \\ 0 & A_{ld} \end{bmatrix}. \quad (20)$$

The plant dynamics and the tracking error can be put into the following form

$$\begin{aligned} \dot{z}(t) &= Az(t) + Bu(t) + Ev(t), \\ e(t) &= Cz(t) + Du(t) + Fv(t), \end{aligned} \quad (21)$$

where

$$E = [0 \quad E_d], \quad F = [-I \quad F_d]. \quad (22)$$

The problem of asymptotic tracking and disturbance rejection is called the output regulation problem. The following theorem gives the solution to the output regulation of linear time-invariant systems.

Theorem1. [15]-[19] Let the feedback gain K_x be such that $A+BK_x$ is exponentially stable. Then, the linear output regulation problem is solvable by a static feedback control of the form

$$u = K_x x + K_v v, \quad (23)$$

if and only if there exist two matrices X and U that satisfy the linear matrix equations

$$\begin{aligned} X A_l &= AX + BU + E \\ 0 &= CX + DU + F \end{aligned}, \quad (24)$$

with the feedforward gain K_v given by

$$K_v = U - K_x X, \quad (25)$$

IV. CONTROLLER DESIGN

To use the linear output regulation design method, the Jacobian linearized model is needed. The dynamic equations of system (1)-(5) are linearized with respect to the unstable equilibrium. The resulting dynamic equations are

$$\begin{aligned} (m+M)\ddot{x} + ml(\ddot{\alpha} \cos \phi - \ddot{\beta} \sin \phi) &= F_x, \\ ml(\ddot{x} \cos \phi + \ddot{y} \sin \phi) + \ddot{\alpha}(ml^2 + I_{Py}) - \alpha mg l &= 0, \\ (m+M)\ddot{y} + ml(\ddot{\alpha} \sin \phi + \ddot{\beta} \cos \phi) &= F_y, \\ ml(-\ddot{x} \sin \phi + \ddot{y} \cos \phi) + (ml^2 + I_{Px})\ddot{\beta} - mg l \beta &= 0, \\ \ddot{\phi}(I_{pz} + I_{Czz}) &= \tau_\phi. \end{aligned}$$

To obtain a linear dynamical model, the system dynamics are presented in the moving body frame by the following coordinate transformations

$$\begin{bmatrix} x_m \\ y_m \end{bmatrix} = \begin{bmatrix} \cos \phi & \sin \phi \\ -\sin \phi & \cos \phi \end{bmatrix} \begin{bmatrix} x \\ y \end{bmatrix}, \quad (26)$$

$$\begin{bmatrix} f_{xm} \\ f_{ym} \end{bmatrix} = \begin{bmatrix} \cos \phi & \sin \phi \\ -\sin \phi & \cos \phi \end{bmatrix} \begin{bmatrix} F_x \\ F_y \end{bmatrix}. \quad (27)$$

The resulting linear dynamic equations are

$$\begin{aligned} (m+M)\ddot{x}_m + ml\ddot{\alpha} &= f_{xm}, \\ ml\ddot{x}_m + \ddot{\alpha}(ml^2 + I_{Py}) - \alpha mg l &= 0, \\ (m+M)\ddot{y}_m + ml\ddot{\beta} &= f_{ym}, \\ ml\ddot{y}_m + (ml^2 + I_{Px})\ddot{\beta} - mg l \beta &= 0, \\ \ddot{\phi}(I_{pz} + I_{Czz}) &= \tau_\phi. \end{aligned} \quad (28)$$

The state vector is defined as

$$\begin{aligned} z_w &= [z_1 \quad z_2 \quad z_3 \quad z_4 \quad z_5 \quad z_6 \quad z_7 \quad z_8 \quad z_9 \quad z_{10}]^T \\ &= [x \quad \dot{x} \quad \alpha \quad \dot{\alpha} \quad y \quad \dot{y} \quad \beta \quad \dot{\beta} \quad \phi \quad \dot{\phi}]^T. \end{aligned} \quad (29)$$

Choosing the exogenous signals to be

$$\begin{aligned} v_1 &= A_m \cos \omega_c t, \quad v_2 = -A_m \sin \omega_c t, \quad v_3 = A_m \sin \omega_c t, \\ v_4 &= A_m \cos \omega_c t, \quad v_5 = bt + m, \quad v_6 = b, \end{aligned} \quad (30)$$

such that the robot tracks a circular reference trajectory of the radius A_m centered at the origin with a constant angular speed of ω_c rad/sec, and a constant spin rate of b rad/sec. Define the system output y

$$y = [z_1 \quad z_5 \quad z_9]^T \quad (31)$$

The tracking error is given by

$$e = \begin{bmatrix} z_1 \\ z_5 \\ z_9 \end{bmatrix} - \begin{bmatrix} v_1 \\ v_3 \\ v_5 \end{bmatrix} \quad (32)$$

From (28), (30), and (32), one can obtain the composite system as follows

$$\begin{aligned} \dot{z} &= Az + Bu \\ \dot{v} &= A_l v \\ e &= Cz + Fv \end{aligned} \quad (33)$$

Based on the linear output regulation design method described in the previous section, we first design a stabilizing controller using the LQR technique. The resulting stabilizing state feedback gain matrix is given by

$$K_z = \begin{bmatrix} K_{11} & K_{12} & K_{13} & K_{14} & 0 & 0 & 0 & 0 & 0 \\ 0 & 0 & 0 & 0 & K_{25} & K_{26} & K_{27} & K_{28} & 0 \\ 0 & 0 & 0 & 0 & 0 & 0 & 0 & 0 & K_{39} & K_{310} \end{bmatrix}, \quad (34)$$

where

$$\begin{aligned} K_{11} &= K_{25} = -223.61, \quad K_{12} = K_{26} = -144.52, \quad K_{13} = K_{27} = -548.81, \\ K_{14} &= K_{28} = -96.16, \quad K_{39} = 223.61, \quad K_{310} = 55.68. \end{aligned} \quad (35)$$

From the plant and ecosystem given in (33), the output regulator equations are given by

$$\begin{aligned} XA_1 &= AX + BU \\ 0 &= CX + F. \end{aligned} \quad (36)$$

By solving (36) for X and U , one can obtain

$$X = \begin{bmatrix} 1 & 0 & 0 & 0 & 0 & 0 \\ 0 & \omega_c & 0 & 0 & 0 & 0 \\ x_{31} & 0 & 0 & 0 & 0 & 0 \\ 0 & vx_{31} & 0 & 0 & 0 & 0 \\ 0 & 0 & 1 & 0 & 0 & 0 \\ 0 & 0 & 0 & \omega_c & 0 & 0 \\ 0 & 0 & x_{73} & 0 & 0 & 0 \\ 0 & 0 & 0 & \omega_c x_{73} & 0 & 0 \\ 0 & 0 & 0 & 0 & 1 & 0 \\ 0 & 0 & 0 & 0 & 0 & 1 \end{bmatrix}, \quad (37)$$

$$U = \begin{bmatrix} u_{11} & 0 & 0 & 0 & 0 & 0 \\ 0 & 0 & u_{23} & 0 & 0 & 0 \\ 0 & 0 & 0 & 0 & 0 & 0 \end{bmatrix}, \quad (38)$$

where

$$x_{31} = \frac{B_{41}\omega_c^2}{-\omega_c^2 B_{21} - B_{21}A_{43} + B_{41}A_{23}}, x_{73} = \frac{B_{82}\omega_c^2}{-\omega_c^2 B_{62} - B_{62}A_{87} + B_{82}A_{67}} \quad (39)$$

$$u_{11} = \frac{\omega_c^2(\omega_c^2 + A_{43})}{-\omega_c^2 B_{21} - B_{21}A_{43} + B_{41}A_{23}}, u_{23} = \frac{\omega_c^2(\omega_c^2 + A_{87})}{-\omega_c^2 B_{62} - B_{62}A_{87} + B_{82}A_{67}} \quad (40)$$

$$A_{23} = \frac{-m^2 l^2 g}{Mml^2 + (m+M)I_{p_{yy}}}, A_{43} = \frac{(m+M)mgl}{Mml^2 + (m+M)I_{p_{yy}}} \quad (41)$$

$$A_{67} = \frac{-m^2 l^2 g}{Mml^2 + (m+M)I_{p_{xx}}}, A_{87} = \frac{(m+M)mgl}{Mml^2 + (m+M)I_{p_{xx}}} \quad (42)$$

$$B_{21} = \frac{ml^2 + I_{p_{yy}}}{Mml^2 + (m+M)I_{p_{yy}}}, B_{41} = \frac{-ml}{Mml^2 + (m+M)I_{p_{yy}}} \quad (43)$$

$$B_{62} = \frac{ml^2 + I_{p_{xx}}}{Mml^2 + (m+M)I_{p_{xx}}}, B_{82} = \frac{-ml}{Mml^2 + (m+M)I_{p_{xx}}} \quad (44)$$

$$B_{103} = \frac{1}{I_{p_{zz}} + I_{C_{zz}}} \quad (45)$$

The linear output regulation controller is

$$u(t) = K_z z(t) + K_v v(t), \quad (46)$$

where

$$K_v = U - K_z X. \quad (47)$$

V. DESCRIPTION OF EXPERIMENTAL SETUP

An experimental setup of the spherical inverted pendulum with an omni-directional mobile robot was constructed as shown in Fig. 3. The mobile robot is driven by three dc motors, which are mounted directly to the omni-directional wheels (equally spaced at 120° from one another). The designed controller is implemented on a DSP board. This DSP board (150-MHz/32-bit) is equipped with a pulse width modulation

(PWM) signal generator and two quadrature encoder pulse (QEP) units. The sampling frequency of the system is chosen to be 1 kHz. The angular displacement of the pendulum is measured by two optical encoders with a resolution of 2000 pulses/rev. The quadrature encoder signals generated by the optical encoders for measuring the angular displacement of the pendulum are connected to the QEP unit on the DSP board. In order to obtain the angular displacement of the wheel for feedback control, an optical encoder with a resolution of 500 pulses/rev is attached to the shaft of each dc motor. The quadrature encoder signals generated by the optical encoders attached to the motors are connected to a QEP circuit that is implemented on an FPGA board. The angular velocities of the pendulum and wheels are estimated from the displacement traveled per unit time and then passed through digital low-pass filters to attenuate the high-frequency noise. The position and orientation of the robot are determined by a dead reckoning algorithm that uses the motor encoder measurements. The PWM signals are generated according to the designed control law and also supplied to PWM driver circuits that drive each dc motor.

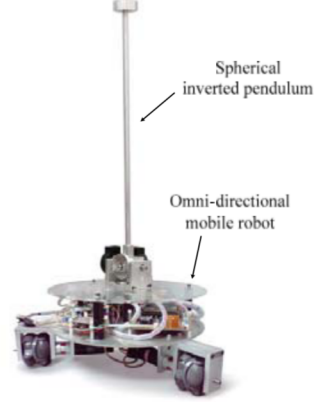


Fig. 3 Experimental setup.

VI. EXPERIMENTAL RESULTS

For validation, the designed control laws were implemented and tested on the experimental setup shown in Fig. 3. The reference inputs are

$$\begin{aligned} v_1 &= 0.8 \cos 0.2\pi t, v_2 = -0.8 \sin 0.2\pi t, v_3 = 0.8 \sin 0.2\pi t \\ v_4 &= 0.8 \cos 0.2\pi t, v_5 = -0.2\pi t, v_6 = -0.2\pi \end{aligned} \quad (48)$$

The initial condition of the system is set to

$$\begin{aligned} z(0) &= [0.8 \ 0 \ 0 \ 0 \ 0 \ 0 \ 0 \ 0 \ 0]^T \\ v(0) &= [0.8 \ 0 \ 0 \ 0.8 \ 0 \ -0.2\pi] \end{aligned} \quad (49)$$

Fig. 4 shows the position responses of the robot. Fig. 5 gives trajectory of the robot in the $X-Y$ plane, and the angular position response of ϕ . In Fig. 6, the angular position responses of α and β are given. The experimental results show that the designed control law is able to stabilize the spherical inverted pendulum system and to track the desired trajectory and orientation. The small-amplitude oscillations of the system

states are possibly caused by the unmodeled dynamics such as friction and slip. A video clip demonstrating the performance of the developed system is available at <https://www.youtube.com/watch?v=i3D3o1N37Ps>. The video shows that the system performs well.

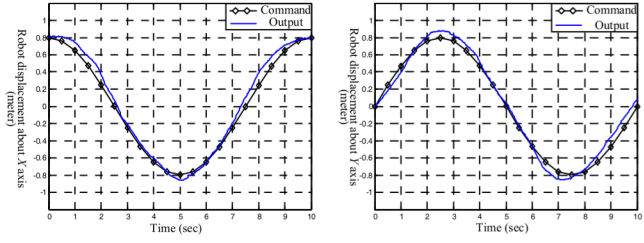


Fig. 4 Experimental results of position responses of the robot with respect to the X -axis and Y -axis.

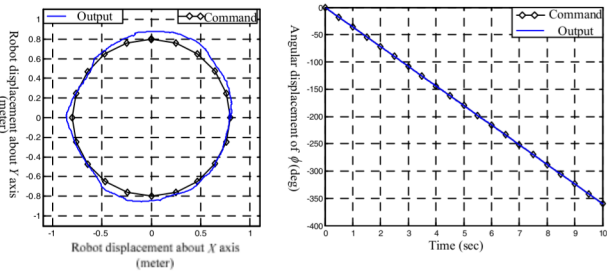


Fig. 5 Experimental results of trajectory of the robot in the X - Y plane, and the angular position response of ϕ .

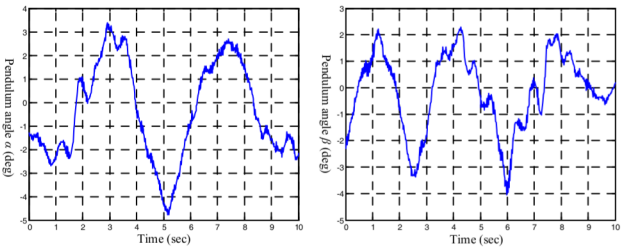


Fig. 6 Experimental results of angular position response of α and β .

VII. CONCLUDING REMARKS

In this paper, an output regulation controller was designed to control a spherical inverted pendulum system actuated by an omni-directional mobile robot for tracking the desired translational trajectory with desired orientation while keeping the inverted pendulum in its upright position. The experimental apparatus was constructed and the control law was implemented. Experimental results were presented to demonstrate the effectiveness of the designed control law. The results showed that the robot is able to track the reference trajectory and reference orientation while balancing the inverted pendulum.

REFERENCES

- [1] A. S. Shiriaev, H. Ludvigsenb, and O. Egeland, "Swinging Up the Spherical Pendulum via Stabilization of Its First Integrals," *Automatica*, vol. 40, pp. 73-85, 2004.
- [2] Inversion Based Control for a Spherical Inverted Pendulum." *International Journal of Control*, vol. 81, pp. 116-133, 2008.
- [3] G. Liu, I. Mareels, and D. Nešić, "Decentralized Control Design of Interconnected Chains of Integrators: A Case Study," *Automatica*, vol. 44, pp. 2171-2178, 2008.
- [4] A. M. Bloch, N. E. Leonard, and J. E. Marsden, "Controlled Lagrangians and the Stabilization of Mechanical Systems I: The First Matching Theorem," *IEEE Trans. Automatic Control*, vol. 45, no. 12, pp. 2253-2270, 2000.
- [5] R. Yang, Y. Kuen, and Z. Li, "Stabilization of a 2-DOF Spherical Pendulum on X - Y Table," *Proc. 2000 IEEE Int. Conf. Control Appl.*, pp. 724-729, 2000.
- [6] L. H. Chang and A. C. Lee, "A Hybrid Controller Design for Bi-axial Inverted Pendulum System," *Int. J. Robust Nonlinear Control*, vol. 19, no. 5, pp. 512-531, 2008.
- [7] R. J. Wai and L. J. Chang, "Adaptive Stabilizing and Tracking Control for a Nonlinear Inverted-Pendulum System via Sliding-Mode Technique," *IEEE Trans. Industrial Electronics*, vol. 53, no. 2, pp. 674-692, 2006.
- [8] B. Sprenger, L. Kucera, and S. Mourad, "Balancing of an Inverted Pendulum with a SCARA Robot," *IEEE/ASME Transactions on Mechatronics*, vol. 3, no. 2, pp. 91-97, 1998.
- [9] K. Watanabe, Y. Shiraishi, S. G. Tzafestas, J. Tang, and T. Fukuda, "Feedback Control of an Omnidirectional Autonomous Platform for Mobile Service Robots," *Journal of Intelligent and Robotic Systems*, vol. 22, no. 3, pp. 315-330, 1998.
- [10] J. B. Song and S. J. Kim, "Design and Control of a Four-wheeled Omnidirectional Mobile Robot with Steerable Omnidirectional Wheels," *Journal of Robotic Systems*, vol. 21, no. 4, pp. 193-208, 2004.
- [11] R. Balakrishna and A. Ghosal, "Modeling Slip for Wheeled Mobile Robots," *IEEE Trans. Robotics and Automation*, vol. 11, no. 1, pp. 126-132, 1995.
- [12] R. L. Williams, B. E. Carter, P. Gallina, and G. Rosati, "Dynamic Model with Slip for Wheeled Omnidirectional Robots," *IEEE Trans. Robotics and Automation*, vol. 18, no. 3, pp. 285-293, 2002.
- [13] J. Wu, R. L. Williams, and J. Lew, "Velocity and Acceleration Cones for Kinematic and Dynamic Constraints on Omnidirectional Mobile Robots," *ASME Journal of Dynamic Systems, Measurement and Control*, vol. 128, no. 4, pp. 788-799, 2006.
- [14] S.T. Kao, W.J. Chiou, and, M.T. Ho, "Balancing of a Spherical Inverted Pendulum with an Omni-directional Mobile Robot," *Proc. of 2013 IEEE Internat. Conf. on Control Appl.*, pp. 760 - 765, Aug. 2013.
- [15] J. Huang, *Nonlinear Output Regulation: Theory and Applications*: SIAM, 2004.
- [16] E. J. Davison, "The Robust Control of a Servomechanism Problem for Linear Time-invariant Multivariable System," *IEEE Transactions on Automatic Control*, vol. 21, no. 1, pp. 25-34, 1976.
- [17] C. A. Desoer and Y. T. Wang, "Linear Time-invariant Robust Servomechanism Problem: A Self-contained Exposition," *Control Dyn. Syst.*, vol. 16, pp. 81-129, 1980.
- [18] B. A. Francis, "The Linear Multivariable Regulator Problem," *SIAM J. Control Optim.*, vol. 15, pp. 486-505, 1977.
- [19] B. A. Francis and W. M. Wonham, "The Internal Model Principle of Control Theory," *Automatica*, vol. 12, pp. 457-465, 1976.
- [20] L. Postelnik, . G. Liu,, K. Stol, and A. Swain, "Approximate Output Regulation for a Spherical Inverted Pendulum," *Proceedings of 2011 American Control Conference*, pp. 539 -544, July 2011.
- [21] Z. Ping and J. Huang, "Approximate Output Regulation of Spherical Inverted Pendulum by Neural Network Control," *Neurocomputing*, Vol. 85, pp. 38-44, May 2012.
- [22] J. H. Ginsberg, *Advanced Engineering Dynamics*, Cambridge University Press, 1995.